Naval Research Laboratory

Washington, DC 20375-5000

NRL Memorandum Report 6815

Flexural Plate Wave Devices for Chemical Analysis

JAY W. GRATE, STUART W. WENZEL* AND RICHARD M. WHITE*

Surface Chemistry Branch
Chemistry Division

**Berkeley Sensor and Actuator Center*
University of California,
Berkeley, California 94720

April 16, 1991

REPORT DOCUMENTATION PAGE

Form Approved
OMB No 0704-0188

1. AGENCY USE ONLY (Leave blank)	2. REPORT DATE	3. REPORT TYPE AND DATES COVERED
	1991 April 16	

4. TITLE AND SUBTITLE

Flexural Plate Wave Devices for Chemical Analysis

5. FUNDING NUMBERS

61-1638-01

6. AUTHOR(S)

Jay W. Grate, Stuart W. Wenzel,* and Richard M. White*

7. PERFORMING ORGANIZATION NAME(S) AND ADDRESS(ES)

Chemistry Division
Naval Research Laboratory
Washington, DC 20375-5000

8. PERFORMING ORGANIZATION REPORT NUMBER

NRL Memorandum Report 6815

9. SPONSORING/MONITORING AGENCY NAME(S) AND ADDRESS(ES)

Office of Naval Technology
Naval Surface Warfare Center
Dahlgren, VA 22448-5000

10. SPONSORING/MONITORING AGENCY REPORT NUMBER

11. SUPPLEMENTARY NOTES

*Berkeley Sensor and Actuator Center, University of California, Berkeley, California 94720

12a. DISTRIBUTION/AVAILABILITY STATEMENT

12b. DISTRIBUTION CODE

13. ABSTRACT *(Maximum 200 words)*

The mass-sensitivities, vapor sensitivities, and vapor detection limits of flexural plate wave (FPW) and surface acoustic wave (SAW) vapor sensors are compared both theoretically and experimentally. FPW devices offer high mass sensitivity at much lower operating frequency. Mass sensitivity increases as membrane thickness decreases; frequency decreases at the same time. This scaling law is in contrast to SAW devices where mass sensitivity increases as frequency increases. FPW devices with sorbent polymer films respond to vapors in a manner similar to SAW devices coated with the same polymer. The FPW vapor sensor, however, offers lower absolute noise levels and hence lower vapor detection limits. It is also demonstrated experimentally that FPW devices can monitor changes in polymer films as the polymer undergoes the glass transition. Plots of frequency vs. temperature show a discontinuity in slope at the static glass transition.

14. SUBJECT TERMS

Vapor sensor
Surface acoustic wave
Flexual plate wave
Glass transition

15. NUMBER OF PAGES

51

16. PRICE CODE

17. SECURITY CLASSIFICATION OF REPORT	18. SECURITY CLASSIFICATION OF THIS PAGE	19. SECURITY CLASSIFICATION OF ABSTRACT	20. LIMITATION OF ABSTRACT
Unclassified	Unclassified	Unclassified	SAR

CONTENTS

FLEXURAL PLATE WAVE DEVICES FOR CHEMICAL ANALYSIS

INTRODUCTION

Flexural plate wave (FPW) devices offer many attractive features for chemical analysis (1-9). As gravimetric sensors for chemical or biological detection, high sensitivity to added mass is achieved at low operating frequencies (typically a few MHz). Both the lithographic fabrication of the device and the design of its oscillator circuit are simplified compared to other acoustic devices operating at higher frequencies. The oscillator circuit can easily be placed remotely from the FPW device. The transducers of the FPW device are placed on the surface of the flexural plate (also referred to as the membrane) which is opposite to the sensing surface, allowing complete isolation of the electronics from the medium being investigated. In addition to their uses as gas or vapor sensors, these devices can be operated in liquids without suffering radiative losses. They also operate well when coated with thick layers (>250 μm) of aqueous gels, including gelatin, agar, poly(vinyl alcohol) and poly(acrylamide) (8). Kinetic effects including the transport of granular solids and the pumping of fluids have also been observed (9).

Figure 1 illustrates the structure of a FPW device. The key feature of the FPW design is the membrane whose thickness is only a few percent of the wavelength of the flexural Lamb wave launched by the interdigital transducers. At a constant transducer geometry, decreasing membrane thickness leads to increasing mass sensitivity and decreasing frequency. Low-loss liquid phase operation is possible because the lowest antisymmetric mode of the Lamb wave in these devices has a phase velocity which is below the compressional sound velocity in most liquids.

Manuscript approved March 7, 1991

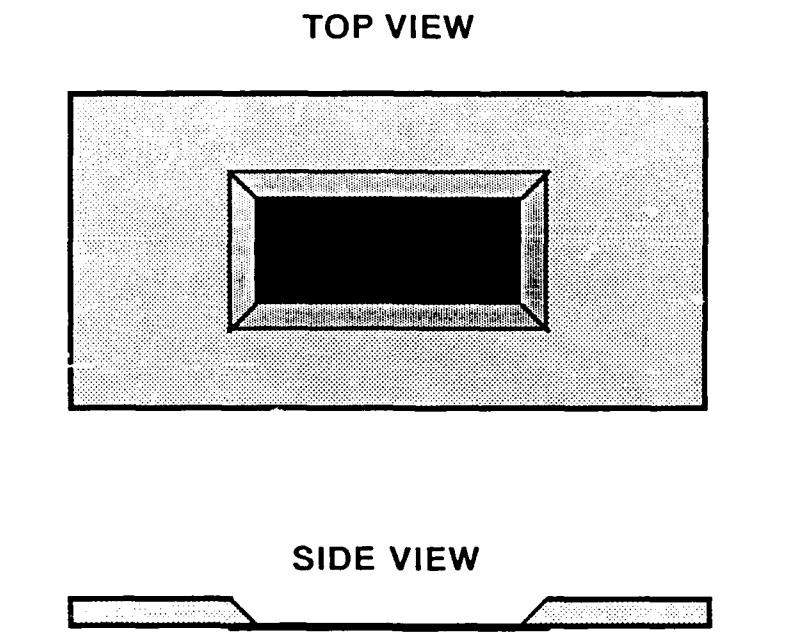

Figure 1. Schematic diagrams of a flexural plate wave device. In the top view, the membrane is shown in black at the bottom of the etch pit. The interdigital transducers are on the opposite side of the membrane, and thus are not shown in this view. The side view and membrane detail show cross-sections through the center. The structures in the membrane detail (shown with exaggerated vertical scale) are, from top to bottom, the supporting silicon substrate on the sides, the silicon nitride layer, the aluminum ground plane, the piezoelectric zinc oxide layer, and the aluminum interdigital transducers. When used as a vapor sensor, the chemically selective sorbent layer would be placed on top of the silicon nitride layer in the etch pit.

When FPW devices are used as vapor sensors in the gas phase, chemical sensitivity is obtained by the application of a chemically selective sorbent film to the upper surface (etch pit side) of the membrane. Sorption of the analyte vapor under isothermal conditions yields a shift in frequency due to the added mass. This method is directly analogous to the piezoelectric sorption detector concept first reported by King in 1964 using the quartz crystal microbalance (QCM), and later extended to surface acoustic wave (SAW) devices, as reported by Wohltjen in 1979 (10,11).

A diagram of a SAW device is shown in Figure 2. SAW devices use interdigital transducers to launch surface Rayleigh waves on a thick piezoelectric plate (typically quartz or lithium niobate). The plate thickness of the SAW device is made many times the acoustic wavelength so that it acts as a semi-infinite medium and energy is confined largely to the surface Rayleigh waves. High mass sensitivity is obtained by increasing the frequency, a scaling law which is quite distinct from that of the FPW device. SAW devices and their uses as sensors have been described in detail in many previous publications (11-23).

In this study, we directly compare the detection of vapors by 5 MHz FPW devices and 158 MHz SAW delay line devices. These SAW devices (20-23) have transducers yielding a 20 μm wavelength on a standard 30 mil (760 μm) quartz plate. The FPW devices were fabricated with transducers yielding a 100 μm wavelength and a 3.5 μm thick membrane. Both devices have high absolute mass sensitivities, but the absolute noise levels of the lower frequency FPW device are substantially lower. Mass sensitivities, vapor sensitivities, and detection limits of FPW and SAW will be discussed using both theoretical scaling laws and practical considerations of sorbent coating thickness, followed by experimental comparisons of vapor detection. In addition, we report for the first time the response of the FPW device to changes occuring in a thin overlay polymer film as it goes through the glass transition.

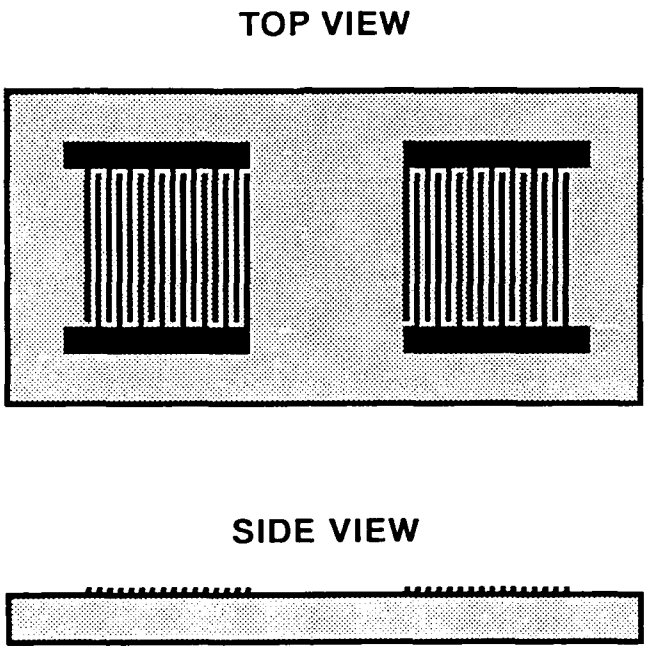

Figure 2. Schematic diagrams of a surface acoustic wave delay line device. The aluminum interdigital transducers are shown in black on the gray quartz substrate. The 158 MHz devices used in this study also have a thin silicon dioxide protective layer (not shown) covering the transducers.

THEORETICAL AND PRACTICAL COMPARISONS OF SAW DELAY LINE AND FPW DEVICE SENSITIVITIES

Sensitivity Concepts. In the discussion below and in Tables I and II, we will compare the sensitivities of FPW and SAW delay line devices, and chemical sensors derived from them. Direct comparisons of these types of acoustic devices are complicated because their designs yield different absolute mass sensitivities, and the scaling laws which govern their mass sensitivities are fundamentally different. In addition, FPW and SAW delay lines as they are normally fabricated operate at different frequencies; their noise levels differ in absolute terms, but are similar relative to their operating frequencies. When used as vapor sensors with chemically selective coatings, comparisons are further complicated by the fact that different film thickness can be applied to each device. As a result, absolute mass sensitivities alone do not necessarily predict vapor sensitivities.

Confusion can also arise from different conventions used to express responses. Some authors express responses as a fraction of the device operating frequency. Thus, the response could be expressed as Hz/MHz, or ppm, and referred to as the fractional frequency response. (The expression ppm as used in this manner must not be mistaken for expressions designating vapor concentrations. In this manuscript all vapor concentrations will be expressed as mg/m^3.) Alternatively, others prefer to report the absolute response, i.e. simply Hz. In an effort to address all readers, we will make comparisons in both fractional frequencies in ppm and absolute frequencies in Hz.

It is also necessary to distinguish between sensitivity and detection limits. The *sensitivity* is the amount of signal change in response to an incremental change in the quantity of analyte present. Mass sensitivity must be further distinguished from the vapor sensitivity of a device with a sorbent coating. The *detection limits* are determined from the signal relative to the baseline noise. A signal-to-noise ratio equal to 3 is often selected to define the minimum detectable quantity or detection limit.

In order to compare mass sensitivities, we define a sensitivity factor, S_m, such that:

$$S_m = \lim_{\Delta m \to 0} \frac{(\Delta V / V_o)}{\Delta m} \qquad (1)$$

where Δm is the uniformly distributed mass per unit area added to the surface of the device (1,3). The added mass could be, for example, due to the deposition of a thin film or the sorption of vapor. V_o is the phase velocity of the device in air before the mass-loading, and ΔV is the change in phase velocity that occurs on mass-loading.

It is customary to use mass-sensitive acoustic devices with a feedback amplifier to form an oscillator whose frequency is measured. If the phase shift of the amplifier is small relative to that of the acoustic device, or if its phase shift is nearly constant with frequency then

$$\frac{F_{loaded}}{F_o} \cong \frac{V_{loaded}}{V_o} \qquad (2)$$

and

$$\frac{\Delta f}{F_o} \cong \frac{\Delta V}{V_o} \qquad (3)$$

where F_o is the fundamental frequency of the oscillator in air, F_{loaded} is the frequency of the oscillator with mass-loading ($F_o + \Delta f$), and V_{loaded} is the phase velocity with mass-loading ($V_o + \Delta V$). The frequency change that occurs on mass loading is given by Δf. (We follow a convention here where the absolute frequency of the oscillator, with or without mass-loading, is expressed with a capital F, while smaller frequency changes are expressed with lower case f. A similar convention will be used with capital M and lower case m mass

per unit areas. This type of convention is not followed with regard to phase velocities.)

Now, when S_m is expressed in terms of frequencies, we obtain,

$$S_m = \frac{(\Delta f / F_o)}{\Delta m} \qquad (4)$$

Thus, S_m expresses sensitivity as the fractional frequency change per incremental change in mass-loading.

S_m is also useful in comparing mass detection limits if the noise levels of the devices being compared are similar in terms of fractional frequencies. This condition is met in the following discussion, assuming a realistic noise level of 1 part in 10^7, or 0.1 ppm for both FPW and SAW delay line devices. This assumption is in accord with experimental noise measurements and previous assumptions made in establishing scaling laws for SAW delay line sensors (12).

FPW Device Mass Sensitivity. The mass sensitivity of the flexural plate wave device is derived from the expression for the phase velocity (V_P) of the zeroth-order antisymmetric (A_o) flexural plate mode

$$V_P = (2\pi/\lambda)\sqrt{B / M_T} \qquad (5)$$

V_P is the phase velocity, λ is the wavelength (determined by the center-to-center distance between adjacent fingers of the interdigital transducers), and B is the effective stiffness of the composite membrane including the effects of in-plane tension (3). M_T is the total mass per unit area of the membrane

$$M_T = M + \Delta m \qquad (6)$$

where M is the mass per unit area of the bare membrane. From eq 1 and eq 5, the mass sensitivity of the bare FPW device in air is given by

$$S_m = -\frac{1}{2M} \qquad (7)$$

For the special case of a single-layer isotropic membrane,

$$M = \rho d \qquad (8)$$

and

$$S_m = -\frac{1}{2\rho d} \qquad (9)$$

where ρ is the density of the membrane material and d is its thickness.

The mass per unit area of the membrane can be easily determined by a liquid-loading method as follows (3,4). When one side of the membrane contacts a liquid with sound velocity V_L greater than the phase velocity V_P, this has the effect of mass-loading the membrane by an amount

$$\Delta m = \rho_L \delta \qquad (10)$$

where ρ_L is the density of the liquid, and δ is the skin depth of the evanescent disturbance in the liquid, given by

$$\delta = \lambda / 2\pi \sqrt{1 - (V_P / V_L)^2} \qquad (11)$$

Eq 5 then becomes

$$V_P = 2\pi/\lambda \sqrt{B / (M + \rho_L \delta)} \qquad (12)$$

(The effective mass-loading is doubled if both sides of the membrane are in contact with the liquid, i.e., $\Delta m = 2 \rho_L \delta$.) Since frequencies and phase velocities are related by eq 2, it can be shown that

$$\frac{F_{loaded}}{F_o} = \sqrt{M / (M + \rho_L \delta)} \qquad (13)$$

With this equation, it is simple to calculate M from the frequencies of the device in air and with one side of the membrane in contact with a liquid of known density and sound velocity, such as water. The device mass sensitivity then follows directly from eq 7. With low viscosity liquids, eq 12 has been demonstrated to be accurate to 0.3% for velocity shifts as high as 36% (3,4). The mass sensitivity determined from the known density and measured thickness of a spin-cast polydimethylsiloxane film was in good agreement with that determined by this liquid-loading method (1).

Eq 7 expresses the mass sensitivity of a bare FPW device in air. If the device has a sorbent coating of mass per unit area m_s the sensitivity to additional mass, e.g. by sorption of a vapor, will be

$$S_m = - \frac{1}{2 (M + m_s)} \qquad (14)$$

Similarly, if the uncoated device is used in a liquid phase, the liquid has the effect of mass-loading the membrane as expressed above in eq 10, and the sensitivity to further added mass will be

$$S_m = - \frac{1}{2 (M + \rho_L \delta)} \qquad (15)$$

This equation assumes the liquid contacts the membrane on one side only (logically the side opposite the transducers). Finally, if the device in the liquid has a coating of mass per unit area m_s, for example a monolayer of biomolecular receptors, its sensitivity to mass which adsorbs to the receptors would be

$$S_m = - \frac{1}{2 (M + \rho_L \delta + m_s)} \qquad (16)$$

SAW Delay Line Mass Sensitivity. The scaling laws for SAW devices have been described in detail elsewhere, and only a few equations will be repeated here (3,12,24). The mass sensitivity expressed as a fractional frequency change has been expressed as

$$S_m = - K(\sigma) \frac{1}{\rho \lambda} \qquad (17)$$

where $K(\sigma)$ is a positive number ranging from approximately 0.8 to 2.2 (typically 1.15) which is a function of the properties of the piezoelectric substrate, ρ is its density, σ is Poisson's ratio, and λ is the wavelength of the surface Rayleigh wave (3).

Converting wavelength to frequency, F_o, eq 17 becomes

$$S_m = -\frac{K(\sigma)}{\rho V_R} F_o \qquad (18)$$

where V_R is the phase velocity of the Rayleigh wave. Wohltjen has expressed the absolute mass sensitivity of the SAW device as

$$\Delta f = (k_1 + k_2) F_o^2 \Delta m \qquad (19)$$

where k_1 and k_2 are constants with negative values related to the properties of the piezoelectric substrate. Eq 19 is valid provided the added mass is non-conducting, and assuming that the added mass does not perturb the frequency by viscoelastic effects. (To avoid confusion, note that in the SAW literature, mass per unit area has usually been expressed as m/A, where m only represents mass.) When eq 19 is rearranged to express SAW delay line mass sensivity in fractional frequencies according to eq 4, then

$$S_m = (k_1 + k_2) F_o \qquad (20)$$

Now it can be seen that eqs 18 and 20 for SAW delay line sensitivity in terms of S_m have the same form.

Although sensors reported to use surface acoustic waves for mass-detection in the liquid phase have been described, the actual nature of the wave responsible for the detection capabilities observed has been the subject of some controversy (18,25,26). Unlike the flexural plate waves, surface acoustic waves suffer radiative losses in liquids. We will not pursue this controversy further here. We do note that an alternative high-frequency device

using horizontally polarized shear waves generated by interdigital transducers in a delay line configuration has been described for mass detection in liquids (27,28).

Theoretical Comparisons of FPW and SAW Scaling Laws. The conventional wisdom on mass-sensitive acoustic devices is that mass-sensitivity increases with the square of the operating frequency. This statement is correct when referring to absolute mass sensitivities (i.e. in Hz) of bulk quartz crystals or SAW devices, as shown in eq 19 for SAW devices. When SAW delay line mass sensitivities are expressed in fractional frequencies, as in eq 18 or eq 20, mass sensitivity increases only linearly with frequency. These expressions more clearly show how detection limits improve with frequency for SAW delay lines since the noise is constant as expressed in fractional frequencies, at least to a first approximation. (Alternatively stated, absolute mass sensitivity in Hz increases with the square of frequency, but the noise increases linearly with frequency, so mass detection limits increase only linearly with frequency.) In fabricating surface acoustic wave delay lines on a given piezoelectric substrate, both the frequency and wavelength are determined by the transducer spacing. Increasing the frequency by decreasing transducer finger spacing is the only way to increase mass sensitivity.

Conventional wisdom for SAW devices cannot be applied to the FPW device. As shown in eq 9 the FPW mass sensitivity is increased by decreasing the plate thickness. At the same time, if the tranducer geometry is kept the same (which is a perfectly reasonable thing to do), the frequency decreases. *Thus, with the FPW device, mass sensitivity can be increased while decreasing the frequency.* This result is completely counter-intuitive to scientists accustomed to thinking about SAW and other mass-sensitive acoustic devices.

Comparisons of Calculated FPW and SAW Mass Sensitivities. To illustrate the above scaling laws in a more concrete fashion, the mass sensitivity of a 5.5 MHz FPW device used in this study is compared with the calculated mass sensitivities of SAW delay lines at various frequencies. The comparisons are presented in Table I. It is

only to simplify matters that we restrict ourselves to a single FPW device configuration in making these comparisons. Other devices with thinner membranes, higher mass sensitivities, and lower frequencies can be fabricated.

The mass sensitivity of the 5.5 MHz FPW device was determined by the liquid-loading method described above. The membrane mass per unit area obtained by eq 13, 1.32×10^{-3} g/cm^2, yields a mass sensitivity S_m of 379 cm^2/g via eq 7. In previous publications, S_m values have been listed in cm^2/g and comparisons in these units are presented in column 3 of Table I. The same S_m values are listed in units of ppm per ng/cm^2 of mass-loading in column 4. Absolute mass sensitivities in Hz per ng/cm^2 are listed in the 5th column. The mass sensitivity of the 5.5 MHz FPW device in fractional and absolute frequencies are -0.379 ppm per ng/cm^2 and -2.08 Hz per ng/cm^2, respectively.

Mass sensitivities for SAW delay lines of various frequencies on ST-cut quartz were calculated by eq 18 and eq 19, using values of -8.7×10^{-8} and -3.9×10^{-8} m^2 s kg^{-1} for k_1 and k_2 (21). Results for a hypothetical 5.5 MHz SAW delay line are given in the second row of Table I. (SAW delay lines are typically fabricated in the range of 30 to 300 MHz.) Its sensitivities in terms of fractional and absolute frequencies are -0.00693 ppm per ng/cm^2 and -0.0381 Hz per ng/cm^2, respectively. These sensitivities are not as good (by a factor of over 50) as those of the FPW device of the same frequency. In order to obain the same absolute mass sensitivity (Hz per ng/cm^2) as the 5.5 MHz FPW device, a SAW delay line on ST-cut quartz would have to be fabricated at 40.7 MHz. Calculations for a SAW delay line at this frequency are given in the 3rd row of Table I. In order to obain the same fractional frequency mass sensitivity (ppm per ng/cm^2) as the 5.5 MHz FPW device, a SAW delay line on ST-cut quartz would have to be fabricated at 301 MHz. Calculations for a SAW delay line at this frequency are given in the 5th row of Table I. Calculations for a SAW delay line at 158 MHz are also given Table I.

Table I. Theoretical Comparisons of the Mass Sensitivity of a 5.5 MHZ FPW Device with ST-Cut Quartz SAW Delay Lines of Various Frequencies

Device	Freq.	Mass Sensitivity			Noise		Detection Limit [a]
		Fractional Freq.		Absolute			
	F_o MHz	S_m -cm^2/g	S_m -ppm/ng/cm^2 [b]	-Hz/ng/cm^2	ppm [b]	Hz	ng/cm^2
FPW	5.5	379 [c]	0.379	2.08	0.1	0.55	0.792
SAW	5.5 [d]	6.93	0.00693	0.0381 [e]	0.1	0.55	43.3
SAW	40.7	51.2	0.0512	2.08	0.1	4.07	5.86
SAW	158	199	0.199	31.4	0.1	15.8	1.51
SAW	301	379	0.379	114	0.1	30.1	0.792

[a] assuming a signal-to-noise ratio of 3.
[b] ppm is fractional frequency, Hz/MHz, not a vapor phase concentration.
[c] determined from the mass per unit area of the membrane, which was determined by the liquid-loading method.
[d] 5.5 MHz is a hypothetical SAW frequency. Actual SAW delay lines are typically in the 30-300 MHz range.
[e] calculated via eq 19.

As noted previously, noise levels for the FPW device and for SAW delay lines are typically 1 part in 10^7, or 0.1 ppm. Using this value, absolute mass detection limits at a signal-to-noise ratio of 3 have been calculated and placed in the last column of Table I. These results for detection limits directly reflect the trends in sensitivity as expressed by fractional frequencies using S_m.

Practical Comparison of FPW and SAW Vapor Sensitivities. Vapor sensitivity, i.e. Hz or ppm per mg/m^3 of vapor in the gas phase, is dependent on the mass sensitivity of the device, the thickness of the coating used to sorb the vapor, and the strength with which the coating sorbs the vapor. The strength of vapor sorption will be considered in terms of the partition coefficient in the next section. In this section, we illustrate the effects of coating thickness, using the term 'thickness' loosely to refer to the amount of coating per unit area of the device surface. The absolute coating thickness can then be expressed in units of length or as the mass per unit area of coating material (m_s). An alternative measure of thickness is the amount of frequency shift, Δf_s, caused by the mass of the coating material on the device surface. This measurement of 'thickness' is relative to the mass sensitivity of the coated device. On SAW delay lines, for example, a 275 kHz coating on a 300 MHz device will have one fourth the absolute thickness (in nm) of a 275 kHz coating on a 150 MHz device, i.e coatings producing a -275 kHz shift in the fundamental frequency F_o.

We will consider two cases in comparing vapor sensitivities of 5.5 MHz FPW and 158 MHz SAW delay lines. First we will compare devices with the same Δf_s of coating material, followed by a comparison of devices with the same absolute amount of coating material. Results are given in Table II.

We chose 275 kHz of coating material for the first comparison based on practical considerations. It has been found (at Berkeley) that a useful guideline for the thickness of sorbent polymer films on FPW devices is to apply an amount which is 10% of the mass per unit area of the membrane itself. This thickness provides good vapor sensitivity without

excessively perturbing the character of the membrane. By this criterion, a coating thickness of 0.132 mg/m3 is indicated for the 5.5 MHz device used in this study (M = 1.32 mg/cm2). This amount is calculated to produce a -275 kHz shift in device frequency due to mass-loading (eq 4).

If a film of identical absolute thickness were applied to a 158 MHz SAW delay line, it would cause a ca. -4 MHz frequency shift according to eq 19. In practice, however, the 158 MHz SAW delay lines and oscillators utilized at NRL are limited to coating thickness of ca. 500-1000 kHz. Soft polymeric films of greater thicknesses result in loss of oscillation due to energy losses into the film. Therefore, 158 MHz SAW vapor sensors (at NRL) are typically fabricated with 200 to 300 kHz of film material. Thus, practical considerations for both the FPW and SAW suggest 275 kHz as a reasonable coating thickness for the first comparison.

Assuming a material density of 1 g/cm^2, 275 kHz of film on the FPW and SAW devices corresponds to absolute film thicknesses of 1320 nm and 87.4 nm, respectively. Thus, the film on the SAW device is only one fifteenth the absolute thickness of the film on the FPW device. Two consequences result: First, the mass per unit area of vapor sorbed, m_v, will be much greater on the FPW device than on the SAW device. Second, the response time of the FPW may be slower because of the greater time required for the vapor to diffuse into the thicker film.

Quantitive comparisons of vapor sensitivities are given in Table II. Assuming that the coating material absorbs 1% of its mass in vapor on exposure to a 1000 mg/m3 vapor challenge, then the mass per unit area of vapor (m_v) in the 275 kHz films on the FPW and SAW devices would be 1320 ng/cm^2 and 87.4 ng/cm^2, respectively. These vapor mass-loadings would yield identical frequency shifts of 2750 Hz.

Table II. Theoretical Comparisons of the Vapor Sensitivities of Coated 5.5 MHz FPW Sensors and a 158 MHz SAW Delay Line Sensor

Device	F_o	Coating Thickness			Vapor Sorbed [a]	Response to Vapor		S/N [b]	Detection Limit [c]
		Δf_s	m_s		m_v	$\Delta f_v/F_o$	Δf_v		
	MHz	-kHz	$\mu g/cm^2$	nm [d]	ng/cm^2	-ppm	-Hz		mg/m^3
FPW	5.5	275	132	1320	1320	500	2750	5000	0.6
SAW	158	275	8.74	87.4	87.4	17.4	2750	174	17.2
FPW	5.5	18.2	8.74	87.4	87.4	33.1	182	331	9.06

[a] assuming that on exposure to 1000 mg/m3 of vapor, the coating absorbs 1% of its mass in vapor.
[b] signal-to-noise ratio.
[c] assuming a signal-to-noise ratio of 3.
[d] assuming a coating material density = 1 g/mL.

This result is not surprising given the relationship between masses and frequencies known for QCM and SAW mass sensors:(10,21)

$$\frac{m_v}{m_s} = \frac{\Delta f_v}{\Delta f_s} \qquad (21)$$

The same equation is valid for FPW devices as we will show in the next section. Two sensors having the same amount of coating in kHz, i.e. having the same Δf_s, and exposed to the same vapor at the same concentration (causing m_v / m_s to be the same) will give the same absolute response, Δf_v. Therefore, their absolute sensitivities in Hz will be identical.

The sensitivity in terms of fractional frequencies (given in the 7th column of Table II) are greater for the lower-frequency device. Assuming the same noise levels as in Table I, the signal-to-noise ratios for this hypothetical vapor exposure and the corresponding minimum detectable quantities at a signal-to-noise ratio of 3 have been calculated. These results are given in the last columns of Table II. Note that the vapor sensitivities in terms of fractional frequencies predict the trends in signal-to-noise ratios and minimum detectable quantities. The 5.5 MHz FPW vapor sensor in this comparison is expected to be more sensitive than the 158 SAW delay line vapor sensor by a significant margin. However, the SAW sensor could have a significantly faster response time because it has a thinner absolute film thickness

For the second comparison, we consider a FPW sensor with the same absolute film thickness (87.4 nm) as the 158 MHz SAW with 275 kHz of coating. Response times on these two sensors should be the same. The results for vapor sensitivity in this case are shown in the last row of Table II. The mass per unit area of the 87.4 nm film on the FPW device produces 18.2 kHz of frequency shift. As a result, the absolute FPW sensor response to the hypothetical vapor exposure is only 182 Hz compared to 2750 Hz on the SAW sensor. In terms of fractional frequencies, however, the sensitivity of the FPW

sensor is slightly better than that of this SAW sensor. Similarly, the signal-to-noise ratio and minimum detection limit for the FPW sensor in this comparison are slightly better than this SAW sensor at the noise levels assumed.

The above comparisons can be summarized in absolute terms as follows, noting that the primary trade-off is between sensitivity and response time. For sensors with identical kHz of coating, the 158 MHz SAW device has greater absolute mass sensitivity, but the FPW sensor absorbs more vapor mass into its thicker (in nm) film, and the FPW device has lower absolute noise at its lower operating frequency. The first two factors cancel exactly to give identical absolute vapor sensitivity, while the third results in significantly better signal-to-noise ratios and detection limits for the FPW vapor sensor. However, the response time of the FPW sensor may be longer.

When sensors are fabricated with the same absolute amount of coating, their performances will be similar in terms of both response time and sensitivity. In this case, other factors must be used to select the best device for the particular gas phase application being considered. The lower frequency FPW device offers potential advantages in cheaper, simpler oscillators, simpler frequency counters, and the option to place the oscillator circuitry remotely from the sensing device. Experience has shown that high frequency SAW devices operated with oscillator circuits must be plugged directly into the oscillator printed circuit board. Stable oscillation cannot be sustained if long wires are used to connect the SAW device to the oscillator.

Vapor Sorption and the Partition Coefficient. The strength and selectivity with which the coating material sorbs the analyte of interest are critical in determing the sensitivity and selectivity of acoustic mass-sensitive vapor sensors. This factor in vapor sensitivity is independent of the particular acoustic device chosen. The strength of absorption can be described with the partition coefficient, K, which is defined as the ratio of the concentration of the vapor in the sorbent phase, C_s, to its concentration in the vapor phase, C_v.

$$K = \frac{C_s}{C_v} \qquad (22)$$

The frequency shift of a SAW vapor sensor has been related to the partition coefficient by

$$\Delta f_v = \frac{\Delta f_s \, C_v \, K}{\rho} \qquad (23)$$

This equation states that the vapor sensor response depends on the amount of sorbent coating expressed as Δf_s , the concentration of the challenge vapor, and the strength with which it is sorbed (21). The ρ in the denominator is the density of the sorbent coating material. This equation assumes that the frequency changes observed are entirely due to mass-ioading effects.

Note that device frequency does not appear explicitly in this equation for vapor sensitivity. For two devices of different frequency with the same coating material applied in the same 'thickness' in terms of Δf_s, the absolute vapor sensitivity will be the same, as was observed in the previous section. The sensitivity in terms of fractional frequencies will be greater for the lower frequency device.

The same equation can be easily derived for FPW vapor sensors as follows. From the relationships above (see eqs 4, 7, and 14), the expressions for the mass sensitivities of the bare device on coating application ($S_m{}^1$), and the coated device on vapor sorption ($S_m{}^2$), are

$$S_m{}^1 = \frac{(\Delta f_s / F_o)}{m_s} = - \frac{1}{2 M} \qquad (24)$$

and

$$S_m{}^2 = \frac{[\Delta f_v / (F_o + \Delta f_s)]}{m_v} = - \frac{1}{2\,(M + m_s)} \qquad (25)$$

respectively. Dividing these two equations and rearranging, one obtains

$$\frac{m_v \Delta f_s}{m_s \Delta f_v} = \frac{(M + m_s) / M}{F_o / (F_o + \Delta f_s)} \qquad (26)$$

For m_s small relative to M, and Δf_s small relative to F, the right side of the equation is equal to unity. One then obtains eq 21. Eq 23 relating Δf_v to K on the FPW device can then be derived exactly as it was for the SAW device (21).

EXPERIMENTAL SECTIONS

Materials. Poly(vinyl tetradecanal) was prepared from poly(vinyl alcohol) (J.T. Baker Chemical Co.) and tetradecanal (Pfaltz and Bauer, used as received) using HCl as the catalyst, using the procedures described in reference 29. (The properties of poly(vinyl acetals) in general are described in reference 30) The product is a clear rubbery material with a glass transition temperature of 5°C. A density of 0.96 g/mL was determined by flotation in methanol / water mixtures.

Poly(vinyl acetate) and poly(isobutylene) were obtained from Aldrich, and poly(t-butyl acrylate) was obtained from Polysciences.

The liquid organic solvents used to generate vapor streams were commercial chemicals of 99% or greater purity, except nitromethane (Fisher certified ACS, Assay 95.4%).

FPW Devices. The FPW devices were fabricated as described in references 5 and 6. The membranes consisted of a 2.3 μm silicon nitride layer, a 0.2 μm aluminum ground plane, and a 1 μm ZnO piezoelectric layer. The interdigital transducers were fabricated with 25 μm fingers and 25 μm spaces in between, giving a 100 μm wavelength. These devices operated at 5.5 MHz and are the devices referred to in the Introduction (3.5 μm membrane) and in the Theoretical section. Devices with 2.0 μm silicon nitride layers and 0.7 μm ZnO layers operating at ca. 4.9 MHz were also fabricated and used in this study. Each device was mounted in a small machined stainless steel chamber with four SMB coaxial feedthroughs. Gold wires were soldered to the contact pads of the FPW device and soldered to the feedthroughs. Feedthroughs were connected to a separate feedback amplifier circuit with RG174U cables and SMB fittings.The stainless steel chamber was fitted with a teflon lid with inlet and outlet tubes. The total gas phase volume inside the mounting chamber is approximately 4.5 mL.

The FPW device was operated as the resonating element in the feedback amplifier circuit, also referred to as the oscillator. The interdigital transducers were driven differentially relative to the ground plane. The circuit consists of a one stage Motorola MC1733 differential video amplifier and a buffer amplifier. No matching circuit was used. Power (+/- 6 VDC) was supplied by a Micronta adjustable dual-tracking DC power supply.

SAW Delay Line Devices. The 158 MHz SAW dual delay line devices and oscillators used in this study were described in detail in reference 21 and also reported in references 20, 22, and 23. These SAW devices have two delay lines on one ST-cut quartz chip, mounted on a TO-8 header. The interdigital transducers are aluminum and they are covered with a protective layer of silicon dioxide (ca. 20 nm). The oscillator circuitry allows the individual delay line frequencies and their difference frequency to be monitored. Power (5 VDC) was supplied by a Micronta adjustable dual-tracking DC power supply. In this study, both delay lines were coated with poly(vinyl tetradecanal) and the individual frequency of one delay line was monitored. Thus, it was operated as a single delay line device. The device was covered and sealed with a nickel-plated lid with two stainless steel tubes for gas flow inlet and outlet. The gas phase volume inside this sensor package is approximately 0.3 mL.

Polymer Film Application. Spray-coated polymer films were applied to the FPW and SAW devices using an airbrush supplied with compressed dry nitrogen and a dilute solution of the polymer (1-10 mg/mL) in HPLC grade chloroform (Aldrich). The oscillator frequency was monitored during deposition; the change in frequency provides a measure of the amount of material applied. To begin coating, the airbrush was placed several inches away from the device and spraying was initiated with the nozzle directed away from the device. Then the spray was passed over the device several times, followed by a pause to observe the change in frequency. This process was repeated many times until the desired frequency change was obtained.

Spray-coated films were examined by optical microscopy with a Nikon Optiphot M microscope using reflected light Nomarski differential interference contrast. Films on the FPW device causing on the order of 250 kHz of frequency change, or ca. 1 μm thick, completely covered the membrane surface. The polymer surface was visibly rough. Films of 250 kHz on the 158 MHz SAW device do not completely cover the device surface. The polymer is present in overlapping circular domains. The film thickness estimated for such films from the kHz of frequency shift and the polymer density, e.g. about 100 nm or less, represent only an average thickness that would be obtained if the film were cc. 'nous and uniform.

Polymer films applied to e FPW device to investigate the ability of the device to observe changes in polymer physical properties as temperature is varied were annealed at temperatures well above their glass transitions for at least several hours under flowing dry nitrogen.

Device temperature control. The mounted FPW device was placed on the bottom of a brass box suspended in a Neslab refrigerated circulating water bath with a programmable digital temperature controller. Foam insulation was placed over the mounting chamber. The oscillator circuitry was located outside the brass box. Carrier gas or vapor streams were routed from their source through a four foot section of 1/8" OD 1/16" ID Ni tubing coiled in the water bath before being fed into the teflon cap on the mounting chamber (to be sure the gas stream would be isothermal). The water bath was operated at 25°C for isothermal measurements of noise or vapor response. Temperatures were monitored with a Cole Parmer Thermister Thermometer (Model N-08502-16) and YSI 427 small surface probes placed on the outside of the FPW stainless steel mounting package or the underside of the SAW TO-8 package. The 158 MHz SAW device and its oscillator and buffer amplifier circuitry were configured so that they could all be placed in the brass box with the lid of the SAW device pressed against the side of the box.

For thermal drift and polymer film characterization measurements, the water bath was programmed to ramp the temperature linearly at a rate of 10 °C/hour. Routine thermal drift measurements on bare devices and the poly(vinyl butyral) coated device were carried out over a temperature range of 15 to 45°C.

Frequency Data Collection. Frequency measurements were made using Phillips PM6674 frequency counters with TCXO, transferring the data to a microcomputer using the IEEE-488 bus. FPW device frequencies were collected at 0.1 Hz resolution. SAW individual delay line frequencies were collected at 2 Hz resolution. Routine noise measurements on FPW devices were typically determined from frequency data collected for 15 min at 4 points per minute. The noise was taken as the standard deviation of the residuals of the linear least squares line through the data. Usually 10 to 20 such measurements were conducted consecutively. During vapor exposure experiments, baseline noise was determined using baseline frequency data collected at 5 points per min for 10 min prior to vapor exposure.

Signal amplitudes measured during FPW/poly(isobutylene) temperature ramping experiments were measured using a LeCroy 9400 Digital Oscilloscope and recorded manually.

Vapor Exposure Experiments. Vapor streams were generated from bubbler sources and diluted using a Microsensor Systems VG-7000 vapor generation instrument. The bubblers were maintained at 15°C in machined aluminum blocks with inlets and outlets for water from a refrigerated circulating water bath. The carrier gas for bubbler vapors was dry nitrogen supplied to the bubblers at 120 mL/min with electronic flow controllers. The saturated bubbler vapor streams were diluted by the VG-7000 using a pulse-width modulation method which we describe in detail in reference 31. The experiments in this paper were all conducted with the saturated (at 15°C) vapor streams diluted by a factor of 4. Finally, the instrument output can be either the diluted vapor stream or clean carrier gas, each at a flow rate of 120 mL/min.

Saturated vapor streams were calibrated gravimetrically by trapping the vapor in tared glass tubes containing activated charcoal and molecular sieves in series. These calibrations were in agreement with vapor concentrations calculated from published vapor pressures and the ideal gas law.

The VG-7000 was connected to a Macintosh computer with a serial communications line. We delivered commands for each experiment using a communications program (Smartcom II); sequences of experiments were programmed using the macro or "autopilot" capabilities of this program.

Experiments to determine equilibrium responses to vapors were carried out by first generating and equilibrating a vapor stream for 45 min while delivering clean carrier gas to the sensor. Vapor was then delivered to the sensor for 5 min, followed by 10 min of clean carrier gas for sensor recovery, another 5 min of vapor to check response reproducibility, and another 10 min of clean carrier gas. Thus each experiment takes 75 min. Sensor frequency data were collected every 12 sec beginning 10 min prior to the first vapor exposure. The two consecutive exposures were quite reproducible. For the organic vapors at the concentrations reported in this paper, sensors coated with poly(vinyl tetradecanal) responded to >90% of response within two data points after the beginning of the exposure, and recovered in a similar period of time when the vapor stream was replaced with clean carrier gas.

Before each 75 min experiment described above, a 75 min control experiment was run to insure that no residual vapors were present in the instrument that could cause a sensor response. The carrier gas flows and timing of the control experiment are identical to those of the subsequent vapor experiment, except that the bubbler is bypassed. The 45 min equilibration time of the control experiment serves to flush out traces of the past vapor which may have adsorbed to tubing walls; following the sensor frequency during the subsequent vapor/clean carrier gas output cycles of the control experiment provides an experimental determination that the system has been flushed.

As a further quality check, a 158 MHz dual delay SAW vapor sensor whose response characteristics are well-known to us (at NRL) was always placed in series after the experimental sensor and its responses were monitored. The consistent responses of this sensor from data set to data set confirmed that the programmed vapor streams were being generated and delivered.

RESULTS AND DISCUSSION

Device Characterization. Before conducting vapor exposure experiments, FPW devices were evaluated for their membrane mass per unit areas, mass sensitivities, noise, and temperature drift. The membrane mass per unit area and mass sensitivities were determined by the liquid-loading method as described above, using water. Values for a device operating at 5.5 MHz were reported above and in Table I; the membrane mass per unit area was 1.32 mg/cm^2, yielding a mass sensitivity of -2.08 Hz/ng/cm^2.

Typical noise levels for bare FPW devices under flowing nitrogen (50-120 mL/min) at 25°C are 0.4 to 0.7 Hz. One of the devices in this study gave noise levels of 0.2 to 0.5 Hz. These results are consistent with previous measurements (1) and with the assumption of 0.1ppm (i.e. 0.5 Hz for a 5 MHz device) in the Theoretical discussion. When polymer coatings are applied, noise levels below 1 Hz are usually maintained, 0.4 to 0.8 Hz noise is typical. The worst case for a polymer coated FPW device in this study was 1 to 2 Hz noise. The results for a poly(vinyl tetradecanal)-coated device are reported in Table III. These noise levels were calculated from baseline frequency data collected prior to each pair of vapor exposures.

For comparison, the noise levels of coated or uncoated 158 MHz SAW devices are typically in the range of 10 to 20 Hz. This result is consistent with the assumption of 0.1 ppm (i.e. 16 Hz for a 158 MHZ device) noise in the theoretical discussion. The best noise levels we have observed on these SAW devices are ca. 5 Hz. The best levels are most likely to be observed for devices operated as single delay lines with many days of operation after coating. On the other hand, noise levels of 30 to 40 Hz are sometimes observed when these SAW devices are operated as dual delay lines with one side bare and the other side freshly coated. Bowers and Chuan have pointed out that cross-talk can occur between the delay lines of the 158 MHz dual delay line SAW device, which contributes to baseline instability (22). These authors report noise levels of 0.1 ppm when these devices are

operated as single delay lines (with the second delay line damped out with excess soft coating). Rezgui and Alder have reported noise levels of 5 Hz for the 158 MHz device (23). The noise levels we observed on the poly(vinyl tetradecanal)-coated SAW device used in this study are reported in Table III. These noise levels of 5-7 Hz are the best that can be obtained from these devices, based on our experience at NRL.

The effect of temperature on FPW device frequency was determined in the range of 15 to 45°C as described in the Experimental Sections. Plots of frequency vs. temperature were linear for bare devices and for the poly(vinyl tetradecanal)-coated device. The temperature drift of a bare device operating a 5.5 MHz was -240 to -270 Hz/°C, or ca. -45 to -50 ppm/°C. On another device operating at 4.9 MHz, the observed drift was in the range of -580 to -640 Hz/°C, or ca. -120 to -130 ppm/°C. With the poly(vinyl tetradecanal) film, the drift of the 4.9 MHz device was -1000 to -1100 Hz/°C. For comparison, the temperature drift of an individual delay line on the 158 MHz SAW device as it is packaged on the TO-8 header is typically -1000 to -2000 Hz/°C or ca. -6 to -12 ppm/°C (22,23). No effort has yet been made to reduce the temperature drift of the FPW device.

Vapor Detection. Vapor sensors were prepared from the FPW and SAW devices by applying a thin film of poly(vinyl tetradecanal). This material was chosen because vapor diffusion through the material is rapid (it is above its glass transition temperature at 25°C) and because it has excellent adhesion to surfaces. (A closely related polymer, poly(vinyl butyral) is used in bonding safety glass.) The FPW device was coated with an amount producing -253 kHz of frequency shift, while the SAW device was coated with an amount producing -247 kHz of frequency shift. Thus, the comparison being investigated experimentally is the case in which the two devices are coated with the same amount of coating in kHz. In absolute terms, the FPW coating is thicker than the SAW coating as discussed previously.

The responses of these devices to several organic vapors were determined as described in the Experimental Sections. The noise levels, responses, and partition coefficients calculated according to eq 23 are tabulated in Table III. In addition, the responses to 1,2-dichloroethane are shown as typical examples in Figure 3; the responses approximate step functions. The equilibrium reponse levels of the FPW and SAW sensors are quite similar; the prediction that devices coated with the same amount of coating in kHz will give the same absolute response is clearly validated. In addition, these results demonstrate that the response mechanism of the FPW vapor sensor is the same as that of the SAW vapor sensor , i.e. sensitivity to the vapor which is absorbed by the applied coating. The noise levels of the FPW device are ca. 10 times lower than those of the SAW sensor, indicating that the FPW sensor should be capable of lower detection limits.

The response times of the two sensors in these experiments were indistinguishable; data points were collected every 12 seconds and both sensors responded to >90% of response within 1 to 2 data points. In an attempt to better distinguish response times, an experiment collecting data every 2 seconds during an isooctane exposure was conducted. The SAW sensor was placed in series immediately after the FPW device so that a faster response on the SAW sensor would unambiguously demonstrate that the FPW sensor was slower, as might be expected from its thicker coating. However, the two sensors' responses were again indistinguishable, requiring 8 to 10 seconds to reach >90% response. It seemed likely that the limiting factor in this experiment was the mixing of the incoming vapor stream with the dead volume of the FPW mounting chamber(ca. 4.5 mL); the reponses of both sensors followed this mixing process. Therefore an insert was prepared to reduce the dead volume directly above the FPW device, and another experiment was run collecting data every 2 seconds. Now the FPW sensor response time was reduced to 2 data

Table III. Performance of Poly(vinyl tetradecanal)-Coated FPW and SAW Devices as Vapor Sensors

Device Type		FPW	SAW	FPW	SAW	FPW	SAW
Freq., MHz		5	158	5	158	5	158
kHz Coating		253	247	253	247	253	247
Vapor	Concn, mg/m3	Noise,[a] Hz		Responses, Hz		Responses, log K	
isopropanol	17520	0.6	6	1822	1697	2.60	2.58
		2.1	14	1801	1703	2.59	2.58
isooctane	44980	0.3	5	7905	8467	2.82	2.86
		0.6	11	7895	8461	2.82	2.86
nitromethane	16450	1.0	5	1504	1369	2.54	2.51
		0.4	7	1511	1453	2.54	2.54
1-butanol	3768	0.8	4	2704	2641	3.44	3.44
		0.3	7	2701	2824	3.43	3.46
1,2-dichloroethane	65080	1.0	4	10846	10735	2.80	2.81
		0.5	7	10850	10776	2.80	2.81
toluene	21220	0.3	6	14977	14568	3.43	3.43
		0.8	5	15263	14966	3.44	3.44
2-butanone	53380	0.4	6	5615	5502	2.60	2.60
		0.7	5	5627	5555	2.60	2.61

[a] The first noise value reported for each vapor is actually the value determined from the control experiment prior tc the vapor experiment. The second value is from the baseline prior to the first vapor exposure of the vapor experiment.

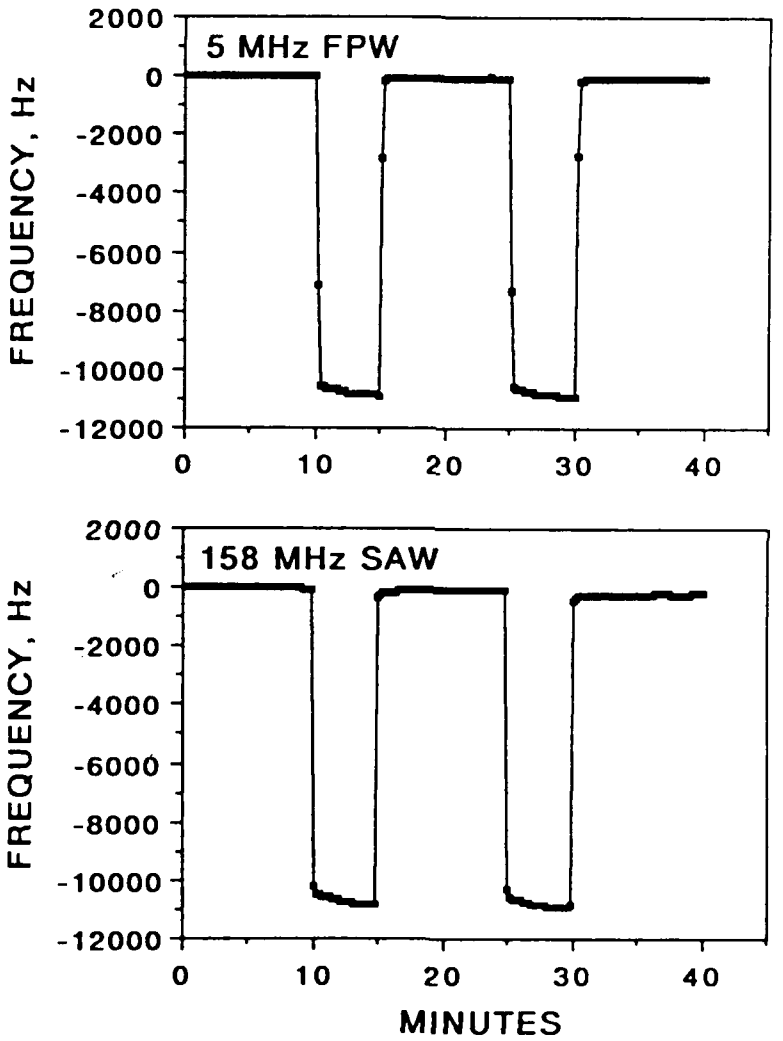

Figure 3. Responses of the poly(vinyl tetradecanal)-coated FPW and SAW sensors to 1,2-dichloroethane at 65080 mg/m^3. Each sensor is coated with ca. 250 kHz of polymer, resulting in very similar equilibrium responses to vapors.

points to >90% response. Similarly, if the SAW device was placed first in series, its response reached >90% in 2 data points. These experiments showed that diffusion into the poly(vinyl tetradecanal) coatings was very rapid, and that we were unable to define experimental conditions where the vapor diffusion into the coating was the limiting factor in the observed response times.

Polymer Glass Transition. We were curious to see how the FPW device would react to changes in the physical properties of the polymer film applied to the membrane. Several physical properties change at the polymer glass transition. There is a discontinuity in the rate of thermal expansion. The free volume is greater above the transition and the density is less above the transition. The glass transition can be probed in bulk samples by measurements of sound velocity, and changes in the properties specifically mentioned above are *frequency-independent* (32-35). The sound velocity through polymer samples decreases with decreasing density or increasing free volume of the material. The modulus, which is strongly dependent on the density, also decreases above the static transition temperature in sound velocity experiments.

Molecular relaxations also occur in polymers as they go through the glass transition. These relaxations are *frequency-dependent.* In the absence of an applied frequency, increased chain segmental motion and polymer softening occur at the usual glass transition, referred to as the static or dilatometric glass transition. When a frequency is applied, the temperature of the primary relaxation occurs at a temperature which is higher than the static glass transition. This is also referred to as the glass transition, which can cause some confusion. Molecular relaxations are usually probed in bulk samples by measurements of sound absorption or by dynamic mechanical methods (32,36). The higher the applied frequency, the higher the temperature required to obtain the relaxation. Relaxation is accompanied by a large change in modulus and a loss maximum. The viscoelastic behavior associated with these relaxations has been modeled with springs and dashpots in the past.

The use of SAW devices to probe polymer glass transitions and relaxation effects has been reported (11,37-39). The distinctions we make above between frequency-independent and frequency-dependent polymer properties have not yet been adequately covered in the SAW literature, however. It should be noted that studies of polymer films on planar acoustic devices differ somewhat from techniques applied to bulk samples because the film thickness is much less than the acoustic wavelength. In addition, the vertical displacement of the acoustic waves on the SAW devices and on the FPW devices is only in the range of a few nm or less. (Displacements are typically 10^{-5} times the acoustic wavelength on SAW devices (37).)

By selecting homopolymers whose properties are well-known we have been successful in demonstrating that the FPW device can monitor both frequency-independent and frequency-dependent polymer properties. Using poly(vinyl acetate) and poly(t-butyl acrylate) we show below that frequency-independent polymer properties which change at the static glass transition can be observed. We also have results with poly(isobutylene) showing that frequency-dependent relaxations can be observed.

For our initial experiments, we chose to examine poly(vinyl acetate), a well-known material whose glass transition begins at ca. 30°C. (The glass transition occurs over a temperature range which is dependent on the rate and method of measurement. The range is at least several degrees wide; the number reported is usually the onset of the transition, although this practice varies.) A film of this material causing 235 kHz of frequency shift was applied to a FPW device; the film thickness is estimated to be 0.94 μm based on the polymer density of 1.2 g/mL and the FPW device mass sensitivity reported in Table I. The frequency of the coated device was then monitored as a function of temperature in the 10-60°C range; the results are shown in Figure 4. A discontinuity in the slope of the temperature response occurs in the range of ca. 33-36°C, which is within 10°C of the known glass transition for this material. The temperature can be ramped up and down many times and the same results are always obtained. The break in the slope of the

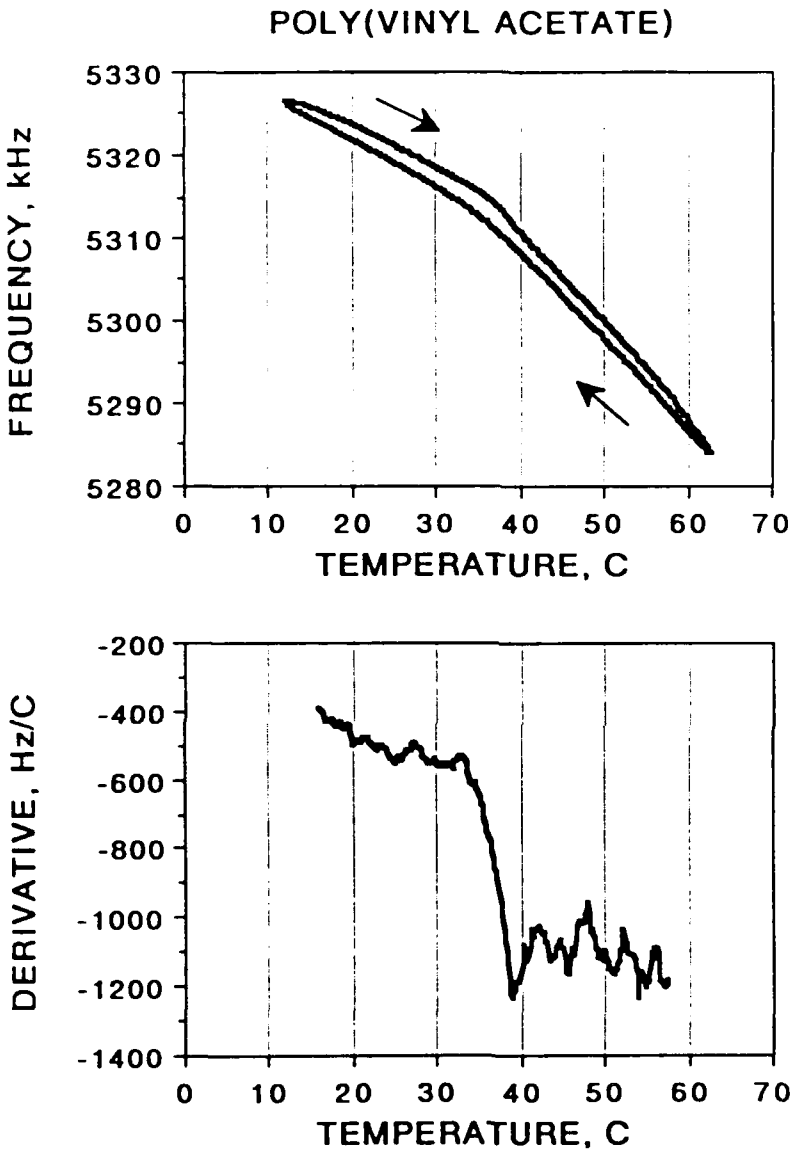

Figure 4. The effect of temperature on the frequency of a poly(vinyl acetate)-coated FPW device, showing the glass transition of the poly(vinyl acetate). The lower plot shows the derivative of the top trace in the upper plot, where the device frequency is being monitored as the temperature is ramped up.

temperature response is slightly sharper when the experiments are run with the temperature ramping up.

The frequency vs. temperature plot in Figure 4 is reminiscent of polymer volume vs. temperature plots. These also appear as lines whose slopes, the rate of thermal expansion, change at the glass transition. When the inherent temperature response of the FPW membrane (-260 Hz/°C for this particular device) is subtracted from the slopes of the poly(vinyl acetate)-coated FPW device frequency vs. temperature plot above and below the glass transition (-1070 and -540 Hz/°C, respectively), one obtains slopes attributable to the polymer film of -810 and -280 Hz/°C, respectively. The ratio of these slopes is 2.9:1. This was an intriguing result because the ratios of the rates of thermal expansion of poly(vinyl acetate) above and below the glass transition which we calculated from published data were 2.6:1 and 2.9:1, depending on the source of the data (40).

This coincidence between FPW device results and thermal expansion coefficients prompted us to look for another polymer whose glass transition falls within the range of our measurement technique (using a water bath for temperature control) and which undergoes a large change in the rate of thermal expansion. We selected poly(t-butyl acrylate) on the basis of data appearing in reference 40, where the glass transition is reported to be 31°C and the rate of thermal expansion above the glass transition is reported to be nearly 4 times that below the transition. Our experimental results from a FPW device with 225 kHz of coating are shown in Figure 5. We observe a discontinuity in slope over a temperature range of approximately 40 to 44°C. This transition was at a somewhat higher temperature than we expected until we examined two other references for the glass transition of poly(t-butyl acrylate); both listed it as 43°C.(41,42) By tracing these references back to the primary literature source, we found that the transition was listed as 40 or 43 °C, depending on the synthetic method used to prepare the polymer.(43) Thus, our results are quite good.

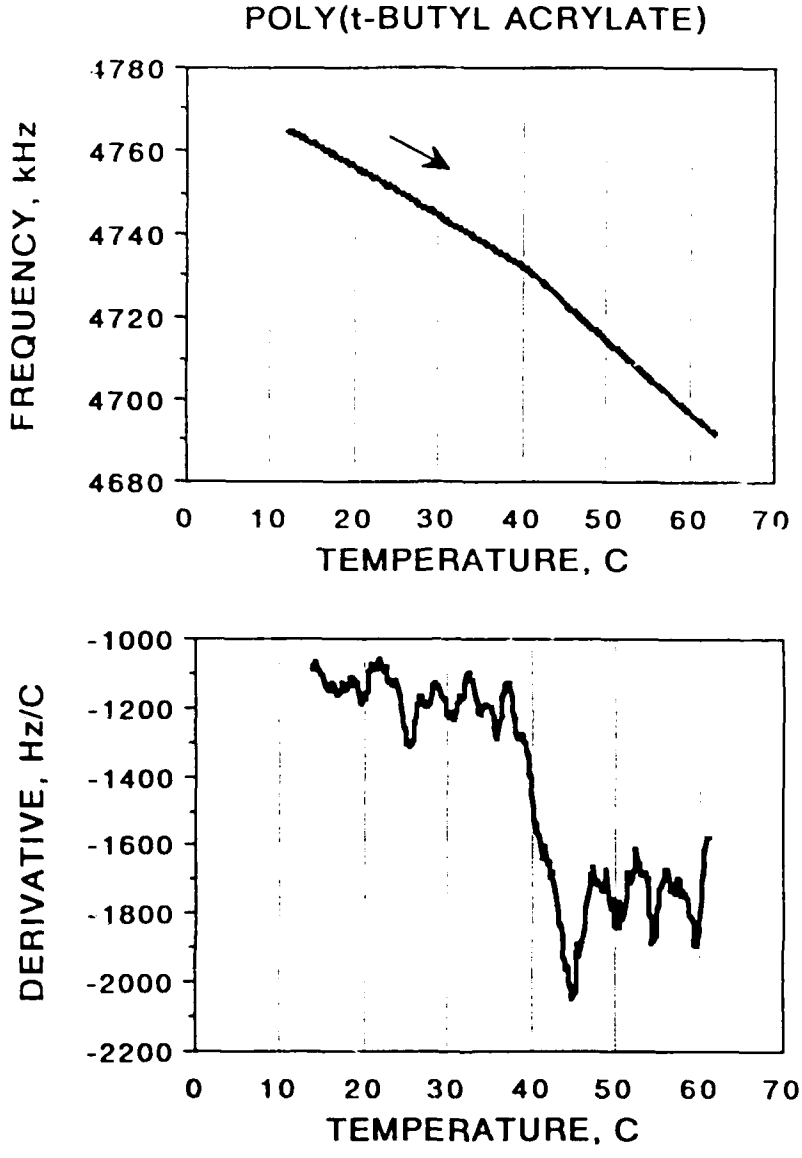

Figure 5. The effect of temperature on the frequency of a poly(t-butyl acrylate)-coated FPW device, showing the glass transition of the poly(t-butyl acrylate). In this case the traces for ramping the temperature up and down were superimposable; the data for ramping the temperature up are shown. The lower plot shows the derivative of the trace in the upper plot.

The inherent temperature response of the bare FPW device which was coated with poly(t-butyl acrylate) was -640 Hz/°C. The slopes with the poly(t-butyl acrylate) coating were -1750 Hz/°C above the transition and -1170 Hz/°C below the transition, giving slopes of -1110 and -530 Hz/°C, respectively, attributable to the polymer. The ratio of these slopes is only ca. 2:1. Assuming that the published rates of thermal expansion are correct, our results for this polymer fail to confirm the simple relationship between FPW results and coefficients of thermal expansion that was suggested by the poly(vinyl acetate) results. This assumption can be questioned, however, because the reference trail on the rates of thermal expansion for this polymer ultimately leads back to a private communication (40,44), and these rates are associated with the rather low glass transition temperature of 31°C. Our ratio of 2:1 is more typical of the results reported for other acrylate and methacrylate ester polymers (40,42).

The above results show clearly that the FPW device is sensitive to those physical properties of polymer layers on the membrane which change at the static glass transition, and that this transition can be observed by following device frequency. (The static glass transition has not been previously observed in experiments following the frequencies of polymer-coated SAW devices.) The precise mechanism for the observed response is not yet clear. The form of the response suggests that volume changes, or the associated changes in polymer density or film thickness are involved, but modulus effects cannot be ruled out. (A change in modulus, however, might be expected to yield a sigmoidal curve in the frequency-temperature plot rather than the simple change in slope observed.) If the FPW device could be used to measure rates of thermal expansion, it would provide a much simpler method than conventional dilatometry. It would require less sample, less sample preparation, and is very easily automated.

In order to observe molecular relaxation effects, we selected a material whose primary relaxation at a frequency of 5 MHz was certain to occur within the temperature capabilities of our experimental apparatus. A previous investigation of poly(isobutylene)

by Ivey et al. shows both sound velocity and absorption as a function of temperature at a variety of frequencies, including 3 MHz and 10 MHz (45). Loss maxima occur at ca. 25°C at 3 MHz and 40°C at 10 MHz, indicating the presence of the frequency-dependent primary relaxation. Sound velocity curves in the same temperature region are non-linear. The static glass transition temperature of poly(isobutylene) is -76°C.

In our first experiment with poly(isobutylene), we coated a device with 260 kHz of material. This amount caused sufficient loss into the film that oscillation at room temperature was somewhat erratic. However, at higher temperatures oscillation was quite stable. On ramping the temperature down from 75°C to 5°C at the usual rate of 10 °C/hour, oscillation stopped at 24°C. On rapidly ramping the temperature back up, oscillation resumed when 30°C was reached. These results show that attenuation is decreasing above ca. 30°C, exactly as expected from the positions of the loss maxima noted above. Moreover, the plot of frequency vs. temperature is not linear, but curved concave upward, *exactly as seen in the previous measurements* of sound velocity in poly(isobutylene) at 3 and 10 MHz.

To more fully examine this material, a FPW device was coated with only 113 kHz of poly(isobutylene) so that oscillation could be sustained through a wider temperature range. This device was ramped from -20 to 100°C repeatedly. The results are shown in Figure 6. We observed the primary relaxation in three ways. First, plots of frequency vs. temperature (at the usual rate of 10 °C/hour) were non-linear, concave upward, and very similar in appearance to the sound velocity vs. temperature curves published by Ivey et al. (see Figure 3 of reference 45). Ivey's sound velocity curves cover a lower temperature range than our experiments and the full curves are sigmoidal in shape. The similarity of the FPW and sound velocity curves in their common temperature range suggests that our FPW curves would also be sigmoidal if we had data at lower temperatures. There is some suggestion of this in the FPW data at the lowest temperatures. The FPW amplitude data support this expectation. Secondly, a peak in the attenuation was

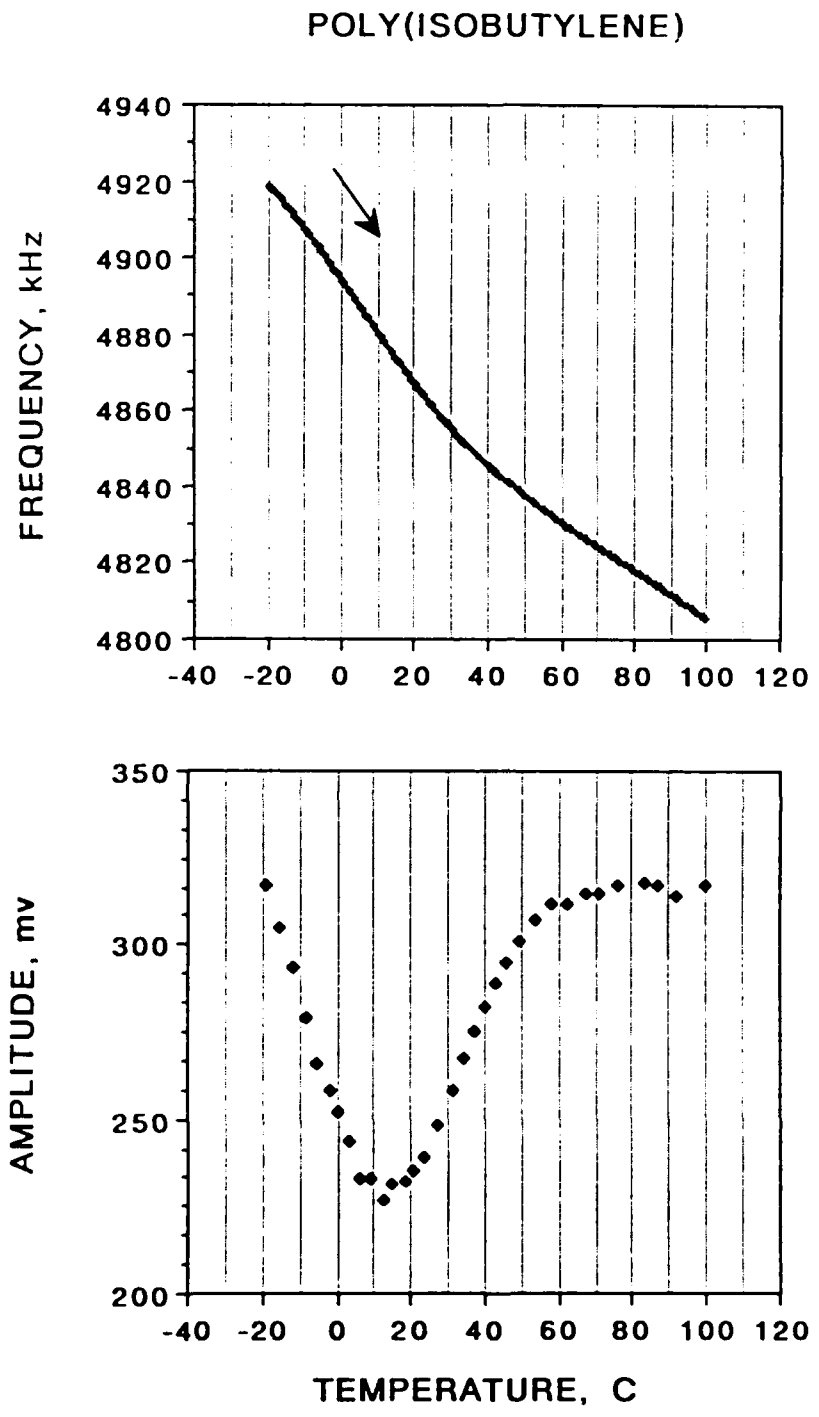

Figure 6. The effect of temperature on the frequency (upper plot) and amplitude (lower plot) of a poly(isobutylene)-coated FPW device, showing the primary relaxation centered near 15°C. The temperature is ramped up in each experiment.

indicated in the range of 8 to 26°C in experiments where the sensitivity of the frequency counter was varied. At the maximum sensitivity, frequencies could be counted throughout the temperature range. At lower sensitivity, frequencies could be counted only between -20 to 8°C, and between 26 to 100°C. The failure to count frequencies in between 8 and 26°C indicated that the signal amplitude had been attenuated, as would be expected if a molecular relaxation occurs in this temperature/frequency domain. Finally, the third line of evidence came from direct measurements of signal amplitude using an oscilloscope. (In this case the ramp rate was increased to 20 °C/hour.) The signal amplitude shows a minimum in the region of ca. 15°C, corresponding to a loss maximum in the polymer material associated with the known primary relaxation.

These types of experiments following both frequency (which measures velocity , see eqs 2 and 3) and attenuation are similar in spirit to those on polymer-coated SAW devices reported by Martin and Frye (39). These authors use a somewhat different experimental apparatus that measures *velocity and amplitude simultaneously.* They demonstrate quite elegantly using both experiment and theory that polymer relaxation processes can be observed on SAW devices. Our results with poly(isobutylene) show that frequency-dependent polymer properties associated with polymer relaxations can also be observed on the FPW device, and the results are quite similar to those obtained from conventional ultrasonic methods on bulk samples.

The results for the three materials above show clearly that both frequency-independent and frequency-dependent polymer properties can be observed with the FPW device. Further investigations on carefully chosen materials of known properties are likely to further elucidate the mechanism of interaction between the flexural Lamb waves and the polymer films. In addition, the development of a theoretical model for the effect of polymer physical properties on these waves is underway (8). It is conceptually interesting to note that the wave/polymer interaction is a two-way interaction: each contributor to the interaction is modified by the other. The polymer affects the wave properties while the

wave affects the temperature at which molecular relaxations occur. At the same time, certain properties of the polymer related to volume changes at the glass transition are not affected.

Final Remarks. The theoretical, practical, and experimental comparisons of FPW and SAW devices carried out above show that there are profound differences between these devices at the same time there are significant similarities. Both can be used as gravimetric sensors for vapor detection. Devices coated with the same amount of coating in kHz provide the same absolute vapor sensitivities, and the relationship between absolute vapor response and the partition coefficient are the same for both devices. However, the FPW device achieves its mass sensitivity at significantly lower frequencies. Lower noise levels obtained at the lower frequency lead to lower detection limits for the FPW device.

Differences between the devices include the fact that their scaling laws are radically distinct. The usual scaling law applied to SAW and QCM devices, i.e., that higher frequencies lead to higher mass sensitivity, is totally inappropriate for the FPW device, where higher mass sensitivity is achieved by *decreasing* membrane thickness and *decreasing* the frequency. FPW devices can be used in liquid phases without suffering radiative losses and with aqueous gels applied (8), while SAW devices cannot. Both devices can be used to monitor polymer properties, but the precise definition of similarities and distinctions in this field will require further experimentation.

FPW devices offer a number of other interesting features for applications in chemical analysis. Their ability to operate in solutions or with gels applied shows clear potential for biosensor applications. Their use in sensing liquid viscosity and density has been reported (2). And recent work shows that these devices can be used to pump fluids and to transport granular solids (9).

ACKNOWLEDGEMENT

This work was supported (at NRL) by the Office of Naval Technology / Naval Surface Warfare Center, Dahlgren, VA, and (at Berkeley) by the Berkeley Sensor and Actuator Center, a National Science Foundation / Industry / University Cooperative Research Center.

REFERENCES

1. Wenzel, S.W.; White, R.M. *Sens. Actuators* **1990**, *A21-A23,* 700-703.

2. Martin, B.A.; Wenzel, S.W.; White, R.M. *Sens. Actuators* **1990**, *A21-A23,* 704-707.

3. Wenzel, S.W.; White, R.M. *Appl. Phys. Lett.* **1989**, *54,* 1976-1978.

4. White, R.M.; Wenzel, S.W. *Appl. Phys. Lett.* **1988**, *52,* 1653-1655.

5. Wenzel, S.W.; White, R.M. *IEEE Trans. Electron Devices* **1988**, *35,* 735-743.

6. White, R.M.; Wicher, P.J.; Wenzel, S.W.; Zellers, E.T. *IEEE Trans. Ultrason., Ferroelectrics, Freq. Contr.* **1987**, *UFFC-34,* 162-171.

7. Chuang, C.T.; White, R.M.; Bernstein, J.J., *IEEE Electron. Device Lett.* **1982**, *EDL-3,* 145-148.

8. Costello, B.J; Wenzel, S.W.; Wang, A.; White, R.M., *IEEE Ultrasonics Symposium,* December 5-7, 1990, Honolulu, HI.

9. Moroney, R.M.; White, R.M.; Howe, R.T., *IEEE Ultrasonics Symposium,* December 5-7, 1990, Honolulu, HI.

10. King, W.H. *Anal. Chem.* **1964**, *36,* 1735-1739.

11. Wohltjen, H.; Dessy, R.E. *Anal. Chem.* **1979**, *51,* 1458-1475.

12. Wohltjen, H. *Sens. Actuators* **1984**, *5,* 307-325.

13. Ballantine, D.S., Jr.; Wohltjen, H. *Anal. Chem.* **1989**, *61,* 704A-715A.

14. D'Amico, A.; Verona, E. *Sens. Actuators* **1989**, *17,* 55-66.

15. Nieuwenhuizen, M.S.; Venema, A. *Sensors and Materials* **1989**, *5,* 261-300.

16. Nieuwenhuizen, M.S.; Barendsz, A.W. *Sens. Actuators* **1987**, *11,* 45-62.

17. Venema, A.; Nieuwkoop, E.; Vellekoop, M.J.; Nieuwenhuizen, M.S.; Barendsz, A.W. *Sens. Actuators* **1986**, *10*, 47-64.

18. Bastiaans, G.J. *Chemical Sensors*; Edmonds, T.E. Ed.; Blackie: Glasgow and London, **1988**, 295-319.

19. Ballantine, D.S., Jr.; Rose, S.L.; Grate, J.W.; Wohltjen, H. *Anal. Chem.* **1986**, *58*, 3058-3066.

20. Rose-Pehrsson, S.L.; Grate, J.W.; Ballantine, D.S., Jr.; Jurs, P.C. *Anal. Chem.* **1988**, *60*, 2801-2811.

21. Grate, J.W.; Snow, A.; Ballantine, D.S., Jr.; Wohltjen, H.; Abraham, M.H.; McGill, R.A.; Sasson, P. *Anal. Chem.* **1988**, *60*, 869-875.

22. Bowers, W.D.; Chuan, R.L. *Rev. Sci. Instrum.* **1989**, *60*, 1297-1302.

23. Rezgui, N.; Alder, J.F. *Analytical Proceedings* **1989**, *26*, 46-48.

24. Auld, B.A. *Acoustic Fields and Waves in Solids*, 2 vols.; Wiley-Interscience: New York, 1973

25. Roederer, J.E.; Bastiaans, G.J. *Anal. Chem.* **1983**, *55*, 2333-2336.

26. Calabrese, G.S.; Wohltjen, H.; Roy, M.K. *Ultrason. Symp. Proc.* **1986**, 607-609.

27. Ricco, A.J.; Martin, S.J. *Appl. Phys. Lett.* **1987**, *50*, 1474-1476.

28. Martin, S.J.; Ricco, A.J.; Niemczyk, T.M.; Frye, G.C. *Sens. Actuators* **1989**, *20*, 253-268.

29. Oguchi, K.; Yoden, T.; Kosaka, Y.; Watanabe, M.; Sanui, K.; Ogata, N. *Thin Solid Films* **1988**, *161*, 305-313.

30. Lindemann, M.K. in *Encyclopedia of Polymer Science and Technology*, Vol. 14, John Wiley and Sons, Inc.: New York, 1971 ; pp 208-239.

31. Grate, J.W.; Klusty, M. NRL Memorandum Report 6762, 1990.

32. Hartman, B. in *Encyclopedia of Polymer Science and Engineering*, Vol 1, 2nd Ed., John Wiley and Sons, Inc.: New York, 1984; pp 131-160.

33. Work, R. *J. Appl. Phys.* **1956**, *27*, 69-72.

34. Wada, Y.; Yamamoto, K. *J. Phys. Soc. Jpn.* **1956**, *11*, 887-892.

35. Kwan, S.F.; Chen, F.C.; Choy, C.L. *Polymer* **1975**, *16*, 481-488.

36. Hadley, D.W.; Ward, I.M. in *Encyclopedia of Polymer Science and Engineering*, Vol 9, 2nd Ed., John Wiley and Sons, Inc.: New York, 1987; pp 379-466.

37. Groetsch, J.A., III; Dessy, R.E. *J. Appl. Poly. Sci.* **1983**, *28*, 161-178.

38. Ballantine, D. S., Jr.; Wohltjen, H. in *Chemical Sensors and Microinstrumentation*, ACS Symposium Series 403, American Chemical Society: Washington, D.C., 1989; pp 222-236.

39. Martin, S.J.; Frye, G.C. *Appl. Phys. Lett.* **1990**, *57*, 1867-1869.

40. Wrasidlo, W. in Advances in Polymer Science, Vol. 13, Springer-Verlag: New York, 1974; pp 29-53.

41. Kine, B.B.; Novak, R. W. in *Encyclopedia of Polymer Science and Engineering*, Vol 1, 2nd Ed., John Wiley and Sons, Inc.: New York, 1984; p 257.

42. Lewis, O.G. in *Physical Constants of Homopolymers*, Springer Verlag: New York, 1968; p 25.

43. Shetter, J.A. *J. Poly. Sci. Part B* **1963**, *1*, 209-219.

44. Kanig, G. *Kolloid Z. Z. Polym.* **1969**, *233*, 829-845.

45. Ivey, D.G.; Mrowca, B.A.; Guth, E. *J. Appl. Phys.* **1949**, *20*, 486-492.